Shear and anchorage behaviour of fire exposed hollow core slabs

Joris Fellinger
TNO Centre for Fire Research, Delft, the Netherlands
Jan Stark
Delft University of Technology, Fac. of Civil Engineering and Geosciences,
Delft, the Netherlands
Joost Walraven
Delft University of Technology, Fac. of Civil Engineering and Geosciences,
Delft, the Netherlands

The fire resistance of hollow core slabs is currently assessed considering flexural failure only. However, fire tests showed that shear or anchorage failure can also govern the load bearing behaviour. As the shear and anchorage capacity of these slabs rely on the tensile strength of the concrete, the load bearing capacity with respect to these failure modes decreases dramatically during fire due to the impact of thermal stresses. This paper presents a FE model for the shear and anchorage behaviour of fire exposed hollow core slabs, comprising new constitutive models for concrete and bond of prestressing strands at high temperatures. The constitutive models were calibrated with 60 new small scale tests carried out at elevated temperatures up to 600 °C. The FE model was validated on the basis of 25 full scale fire tests on hollow core slabs loaded in shear. Finally, a parameter study was carried out with the FE model. The results showed that the thermal expansion of concrete, the ductility of concrete in tension and the restraint against thermal expansion by the supports are the main influencing factors. It is recommended to control these factors in design in order to improve the safety level. This paper is an extended summary of the dissertation by the first author [10].

Key words: Fire resistance, shear failure anchorage failure, bond, prestressing strand, FE modelling

1 Introduction

1.1 HC slabs

Hollow core (HC) slabs are made of pre-cast concrete with pre-tensioned strands. The slabs consist of pre-cast units of typically 1.2 m wide. The cross sectional depth depends on the intended span and ranges between 150-400 mm reaching spans up to 16 m. The number and shape of the hollow cores is adjusted to the depth of the slab. These slabs are very popular in offices and dwellings, thanks to the large span to depth ratio. This is a result of the reduction of weight, maintaining the effectiveness of the cross section, due to the hollow cores in combination with a relatively high strength of the concrete, typically C45 to C60.

The HC units are manufactured on long benches, typically 100-200 m in length. First, strands are tensioned along the bench. Subsequently, the concrete is cast automatically by a moulding and casting machine that is moving along the bench. After the concrete has reached sufficient strength, the external pre-stressing force is released and elements of desired lengths are sawn out.
Shear reinforcement or other mild reinforcement is never applied as it would obstruct the movement of the machine. Neither are anchors for the prestressing strands, because they would introduce large splitting stresses and their position should be known accurately before casting.

1.2 ***Problem statement***

At ambient conditions, HC slabs are designed to be simply supported. Walraven and Mercx [20] determined four different failure modes, i.e. flexure, anchorage, shear tension and shear compression.
When HC slabs are exposed to fire, they have to maintain their load bearing and fire separating function for a minimum time as required by Building Regulations. Current design codes for fire design such as Eurocode 2 [16] take only flexural failure into account, while fire tests carried out in the past demonstrated that the other failure modes or combinations of failure modes can also dominate the behaviour. Because there is a lack of fundamental understanding of the shear and anchorage behaviour, an optimum design for both safety and economics can yet not be achieved.
Flexural failure of HC slabs under fire conditions can be assessed on the basis of the theory of plasticity and on the assumption that thermal strains can be neglected. As the production process does not allow for the inclusion of mild reinforcement, both the shear tension capacity and the anchorage capacity rely on the tensile strength of concrete. For such failure modes Eurocode 2 [16] states in Annex D: "*…special consideration should be given where tensile stresses are caused by non-linear temperature distributions (e.g. voided slabs, thick beams, etc). A reduction in shear strength should be taken in accordance with these increased tensile stresses.*"

However, a simple cross sectional analysis of the thermal stresses leads to the conclusion that within 20 minutes of fire exposure the thermal stresses equal the tensile strength, i.e. cracking occurs and according to the Eurocode there would be no shear strength left, see Figure 1.
But in most fire tests, no shear failure occurs at this time. So, there is a need for a better understanding of the impact of thermal stresses on the shear behaviour.

1.3 ***Objective***

The objective of the study is to obtain a fundamental understanding of the shear and anchorage behaviour of fire exposed HC slabs and to develop numerical models to predict this behaviour. With the models, practical recommendations for design can be developed.

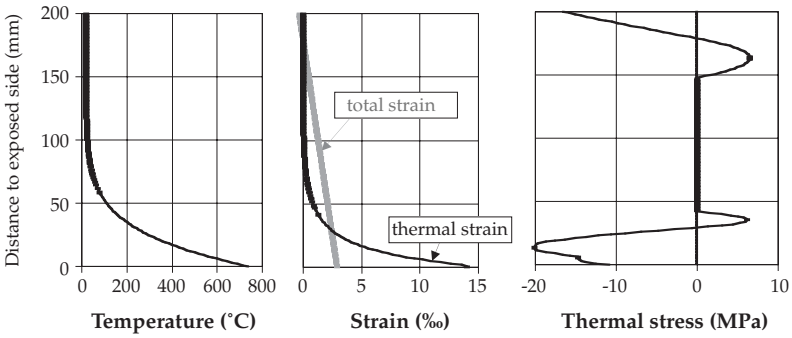

Figure 1. Calculated temperatures, strains and thermal stresses in a 200 mm deep HC slab after 15 minutes of standard fire exposure, calculated on the basis of gravel concrete thermal properties according to Eurocode 2 and assuming prestressing by 8 strands Ø9.3 mm with an initial prestress of 1050 MPa

More specifically, it was postulated that for the assessment of shear and anchorage behaviour, the following phenomena should be taken into account:

- Incompatible thermal strains leading to thermal stresses
- Decomposition of strains in reversible and irreversible parts
- Support conditions that restrain the thermal expansion of the fire exposed slab
- Influence of the applied load on the deterioration of the load bearing capacity during fire
- Relation between the fire safety and the time to failure

The research is limited to HC slabs as defined in the European product standard [15], exposed to standard fire conditions [14] and simply supported on rigid supports like concrete walls. In addition, some attention is paid to the effects of restraint to thermal expansion by the supports.

*1.4 **Approach***

Firstly, the load bearing behaviour at ambient conditions was evaluated. Theoretical formulations of the load bearing capacity with respect to the four failure modes were composed from different sources of literature and then compared with 257 tests at ambient conditions. Secondly, the fire behaviour of HC slabs was assessed on the basis of 80 tests found in literature. It is noted that these tests generally served the commercial goal to demonstrate that a certain fire resistance could be achieved under realistic (and sometimes complex) boundary conditions rather than the scientific goal to observe a failure mechanism under academic (and preferably simple) boundary conditions. With these tests, the failure modes under fire conditions were defined and it was tried to find relationships between various parameters and the observed behaviour.

From the inventory of existing fire tests, it was concluded that there was a need for further testing. Therefore, 25 full scale fire tests on HC slabs were carried out at the TNO Centre for

Fire Research. The fire tests were carried out with the same test set-up with respect to the support conditions and the loading conditions as in the standard shear test as prescribed in the product standard [15].
The tests were also used to develop and validate new finite element (FE) models. Two two-dimensional models were developed. The first model is a model of the cross section. This was used to calculate the temperature distributions, the effect of incompatible thermal strains on the development of splitting cracks and the resulting confining action on the strand by the concrete around the strand. The second model is a model of the entire slab, including the support conditions and the loading. It contains a new plastic constitutive bond model for the interface element between the strands and the concrete. In this model, the bond yield strength depends on the confining action of the concrete cover around the strand as determined with the cross sectional model. Both FE models use a newly composed constitutive model for concrete, based on various literature sources [18],[17],[2],[1],[4], which allows for a dependency of the stress-strain relationship on both temperature and loading history during heating. It also includes the effect of transient creep.
Obviously, the new constitutive models needed calibration. Therefore, 60 small scale tests at elevated temperatures were carried out, on both the concrete properties and the bond properties of the pre-stressing strands. The main parameters were calibrated in a narrow range. With the calibrated values, the FE models were successfully validated against tests on the shear and anchorage behaviour of HC slabs at both ambient conditions and fire conditions. After the validation, a limited parameter study was carried out which is presented in paragraph 4.4.

2 Load bearing behaviour at ambient conditions

At ambient conditions, HC slabs are designed to be simply supported. Walraven and Mercx [20] determined four different failure modes, i.e. flexure, anchorage, shear tension and shear compression, see Figure 2.

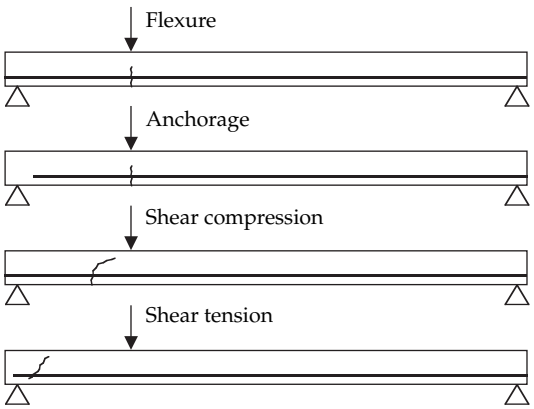

Figure 2. Failure modes for HC slabs at ambient conditions

Flexural failure is the most common failure type and it is the preferred failure type as it is ductile and predictable. It is the result of a bending moment which first leads to the development of one or more flexural cracks, starting at the bottom side of the slab. The slab is designed in such a way that the strands can take over the tensile force that is released in the crack. A further increase of the bending moment will lead to yielding of the strands in one of the flexural cracks which is accompanied with large opening of this crack and large deflection. Ultimately, the slab fails by rupture of the strands. The slab is designed in such a way that rupture of the strands prevails over crushing of the concrete in the compression zone. Anchorage failure can also occur, particularly when the load causes a large bending moment close to the end of the HC slab, near the support. Within this distance from the end of the slab, the so-called development length, the full tensile force required to lead to yielding and rupture of the strands can not be developed due to a lack of bond strength between the strands and the concrete over the embedment length. As a result, the slab collapses as the strands are pulled out. If the flexural crack occurs within a certain distance from the end of the slab, the so-called critical length, the strands will be pulled out immediately at the initiation of a flexural crack. If the flexural crack occurs outside the critical length but within the development length, the strands are not directly pulled out after the formation of the flexural crack, but after some further increase of the bending moment. Rupture of the strands will not occur. After a flexural crack has formed, an additional tensile force arises in the strand due to a change in the load bearing mechanism with respect to the shear force. Immediate pull-out at the onset of cracking has a brittle character whereas pull-out after a further increase of the load shows more ductility. The actual behaviour depends on the loading scheme. If a point load is applied near the support, the brittle mode will dominate, while the ductile mode will dominate for point loads further away from the support, see Figure 3.

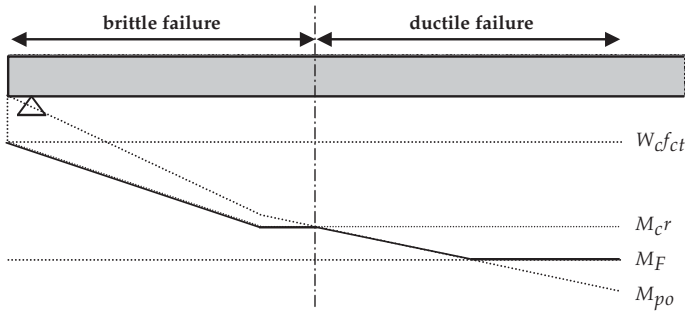

Figure 3. Development of the load bearing capacity against bending moment for flexural failure MF and anchorage failure by pull-out of the strands Mpo or the initiation of the crack Mcr. The continuous line indicates the ultimate capacity, Wc is the section modulus of the slab and fct the tensile strength of concrete.

Shear failure can occur in a cracked cross section, which is called shear compression failure, or near the support in an un-cracked cross section, the so-called shear tension failure. Shear compression failure is limited by the capacity to transfer shear by the concrete in the compression zone. This capacity is enhanced by the pre-stress, by the dowel action of the strands and by the rough crack surface, which is kept relatively closed by the strands. Shear tension failure occurs near the support, where flexural cracks can barely develop as the bending moment is almost zero. The shear stresses lead to a principal tensile stress in the webs which reaches a maximum just outside the zone where the support reaction affects the stress state. When these tensile stresses lead to cracking, no redistribution of stresses is possible as the embedment length of the strands with respect to these cracks is far too short and immediately brittle failure occurs.

It was proven that these four failure modes can be described sufficiently accurate by analytical formulations as given in Eurocode 2 [16] and the Model Code [12]. These formulations were validated by an extended comparison with the load bearing capacity obtained from 257 tests on HC slabs at ambient conditions, carried out in various laboratories over the world. Therefore the analytical formulations could be used to derive the degree of utilisation with respect to each failure mode for HC slabs in fire tests found in literature.

3 Fire conditions

3.1 ***Theoretical background***

Under fire conditions, the load bearing capacity decreases due to the degradation of the material's mechanical properties at elevated temperatures and due to damage caused by thermal stresses. Thermal stresses are caused by a thermal strain field that is incompatible. Strain fields must satisfy compatibility requirements resulting from the fact that six strain components (ε_{xx}, ε_{yy}, ε_{zz}, ε_{xy}, ε_{yz}, ε_{zx}) are obtained from three displacements (u_x, u_y, u_z). When a two-dimensional plane is considered, the compatibility requirement is given as:

$$\frac{d^2\varepsilon_{xx}}{du_z^2} + \frac{d^2\varepsilon_{zz}}{du_x^2} - 2\frac{d^2\varepsilon_{xz}}{du_x du_z} = 0 \qquad \text{Eq. 1}$$

Thus, strains in the axial direction (ε_{xx}) that vary at a higher than linear degree along the depth of the slab (z- direction) must be accompanied by vertical or shear strains in order to satisfy the compatibility requirement.
For structural members with a high span to depth ratio, the vertical strains will be small and shear strains will develop. If the shear stiffness is high, the compatibility requirement results in the fulfilment of Bernouilli's hypotheses that plane cross sections remain plane. This justifies the cross sectional calculation of the thermal stresses shown in Figure 1. In fire exposed

concrete slabs, the thermal strains in the axial direction do vary non-linearly over the depth of the slab. As a result, mechanical strains have to develop to counteract these incompatible thermal strains, in order to result in a linear distribution over the depth of the slab of the total strain in the axial direction, This distribution can be calculated on the basis of the requirement that the resulting displacements and rotations must satisfy the kinematic boundary conditions at the supports. Moreover, the mechanical strains lead to thermal stresses that have to be in equilibrium with the external loads. At the end of a simply supported structural member, no axial stresses can occur. Locally, cross sections are warped and shear strains develop to satisfy the compatibility requirement, see Figure 4.. These shear strains lead to shear stresses that lead to a gradual increase in the axial direction of the thermal stresses. So, the shear stiffness determines the length over which the axial thermal stresses are built up.

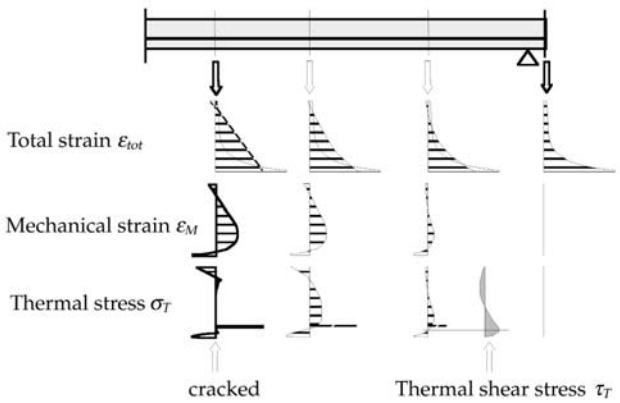

Figure 4. Development of thermal stresses near the end of a simply supported slab

3.2 ***Fire tests obtained from literature***

In literature, 80 fire tests on HC slabs have been found. It appeared that some kind of shear or anchorage failure dominated the load bearing behaviour in about 25 % of the tests, see Figure 5. These failures were in most cases premature, i.e. occurred before the required fire resistance time was reached. The distinction between shear tension, shear compression and anchorage failure could not be made, partly because these tests were poorly reported as all these tests were meant to demonstrate a satisfactory fire resistance rather than to obtain a scientific understanding of the failure behaviour.

A study into the main influence parameters showed first and for all that supports that restrain the thermal expansion in the spanning direction improved the shear and anchorage behaviour significantly. This is just a confirmation of existing knowledge. Secondly, opposite to what might be expect, it was shown that an increase of the axis distance, i.e. the distance from the

centre of the strands to the exposed side, had rather a detrimental than a beneficial influence on the shear and anchorage behaviour. Apparently, the temperature of the strand is not an important indicator. Only if the end zone of the slab was isolated over 500 mm or more, shear and anchorage failure was avoided. Thirdly, shear and anchorage failure is less critical in thinner slabs as such a failure mode appeared only three times in slabs with a depth smaller than 200 mm. Those failures could be attributed to other factors, such as a very high shear loading. Generally, the shear and anchorage failure is more likely if the shear loading is higher. Except for three tests, all tests with a depth of 200 mm or more, without considerable axial restraint and without isolation of the end zone over at least 500 mm, failed if the degree of loading was more than 30 % relative to the actual anchorage capacity at ambient conditions. In these three tests the thermal expansion in the transverse direction was restrained at the support using either a steel belt or a heavily supporting beam that was properly connected to the slab. However, the transverse restraint was not always so effective. Finally, the age of the slab did not seem to play an important role, provided that the slab had an age of more than approximately one month and the moisture content was sufficiently low to avoid critical pore pressures.

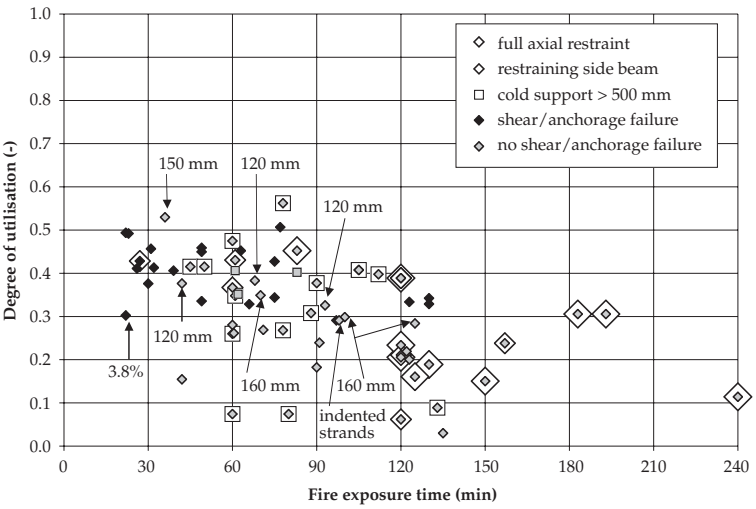

Figure 5. Fire resistance time versus the degree of utilisation with respect to anchorage loading. I.e. the ratio between the anchorage loading during fire and the anchorage capacity at room temperature with respect to the cross section with the highest anchorage loading. The axial restraint was either full or partial, realised by side beams. The degree of restraint is indicated with the size of the marker around the marker indicating the type of failure. The three specimens that did not fail while the anchorage loading was more than 30% and no isolation or restraint was applied are indicated with a grey box rather than a grey diamond. Other specimens that did not fail were either less deep than 200 mm or provided with axial restraint or an isolated support over at least 500 mm. One early failure at 22 minutes might be attributed to the relatively high moisture content of 3.8 %.

3.3 ***New fire tests***

As the existing fire test data did not provide an adequate basis for the understanding of the failure behaviour, 25 new fire tests were carried out. Most of these new tests (21) were conducted on double rib specimens sawn out of HC slab units, with the objective to observe the expected cracking in all webs due to thermal stresses and to measure the slip at the end of the strands during the fire exposure. The webs were visible thanks to the slender isolated steel plate that was used to close off the furnace, see Figure 6. The sawn end surface was accessible with a simple slip calliper.

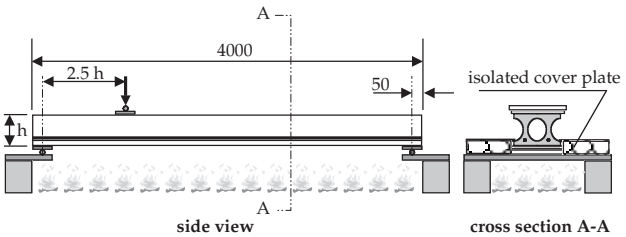

Figure 6. Test set-up for the new fire tests, loaded according to the standard shear test for HC slabs

Some influencing parameters were evaluated: First the geometry was varied, using 4 different types of HC slabs, 200, 260, 265, and 400 mm deep, see Table 1. For the 200 mm deep slab, the axis distance of the strands and the production process were varied. For this type, coincidentally, the same geometry was produced in one plant using an extrusion process and in another plant using a slip form process. For the 260 mm deep slab, the load level was systematically varied with a shear force between 11 and 23 % of the actual shear capacity at room temperature conditions. This capacity was for all fire test specimens obtained as the average capacity of three standard shear tests at room temperature. Finally, the support details were changed relative to the simply supported basic case of Figure 6. Three tests were carried out in which the thermal expansion in the spanning direction was restrained by a hydraulic actuator that simulated a spring with a stiffness of 50 kN/mm. The point of application was positioned at $^1/_4 \cdot h$ from the exposed side for the specimens with a depth of h = 265 and 400 mm and $^1/_2 \cdot h$ for the 200 mm deep specimen. Three more tests on the 260 mm deep specimens were carried out with a reinforced end beam cast in one batch with a concrete filling of the central core over a length of 800 mm with a reinforcing bar of Ø 10 mm, in order to evaluate practical design recommendations [3].

The other tests were carried out on complete single HC units. Three of these tests were conducted using identical units produced in one batch on the same prestressing bench. The fire tests appeared to be very reproducible with a consistent failure behaviour and consistent time to failure, i.e. failure times of 39, 40 and 42 minutes.

Table 1. Overview of the fire tests on HC elements, see Figure 8 for cross sectional shapes of the slabs

depth – # HC (mm)	Production process	axis dist. (mm)	type	Support detail[1]			load level	failure mode[2]			failure time	Remarks
				s	r	e	(%)	S	A	F	(min)	
200 - 7	slip form	40	ribs	s			21		A		96	*no slip measured*
	extrusion			s			16			F	125	$V_u = 30\%$
		44		s			18		A		125	$V_u = 34\%$
					r		18			F	159	$V_u = 37\%$
			unit	s			19			F	117	
260 - 5	slip form	40	ribs	s			23		A		48	
							17		A		45	*fluctuating load*
							11		A		123	$V_u = 16\%$
		[3]		s			23		A		55	
							20	S	A		56	*restarted after 8 min*
							17	S	A		114	
							14	S	A		123	*loading failed*
						e	23	S	A		49	
							20	S	A		50	
							17	S	A		99	
			unit	s			23	S	A		39,40,42	
265 - 4	extrusion	40	rib	s			23	S			35	
					r		23	S			35	
			unit	s			23	S			33	
400 - 4	extrusion	[4]	rib	s			23	S			60	
				s			30	S			24	*low quality core filling*
			unit	s			23	S			33	

1) (s) = simple supports, (r) = restraint in spanning direction, (e) = reinforced end beam

2) (S) = shear failure, (A) = anchorage failure, (F) = flexural failure

3) Strand position: 4x12.5–40 + 2x12.5-76 4, for the double ribs: 1x12.5-40 + 1x12.5-76

4) Strand position: 6x9.3–40 + 2x9.3-73 + 5x12.5-40 + 3x12.5-88, for the double ribs: 4x9.3-40 + 1x12.5-40 + 1x12.5-88

In all specimens, even in the restrained ones, thermal cracks developed in the webs on a regular distance over the entire span already within 14-16 minutes, see Figure 7. These cracks were first suggested by Prof. dr. ir. M. Fontana of ETH Zurich in an international technical meeting of ECCS-IPHA and now demonstrated by the author. Near the loading point, the cracks were slightly inclined, indicating some effect of the loading on the crack propagation. Moreover, splitting cracks developed around most strands, see Figure 8, which gives an overview of the observed crack patterns in all investigated types of HC slabs. In the 265 mm deep slabs, horizontal cracks developed through the smallest web section over almost the entire length. Also the slip of the strands increased rapidly directly from the start of the fire both at the loaded and unloaded end of the specimens, see § 4.3, indicating that the slip is driven by the thermal expansion.

Figure 7. Thermal cracks in the web of a 200 mm deep slab after 20 minutes of fire exposure

In case flexural failure dominated, the vertical crack in the web below the loading point grew into a flexural crack and opened until rupture of the strand occurred. In case anchorage failure dominated, the strand was pulled out. In case shear failure occurred, the horizontal cracks grew together with the vertical cracks and one large combined crack from the loading point to the nearest support opened up to failure. Near collapse, also significant slip of the strands developed. In case of combined shear and anchorage failure, horizontal splitting cracks through the web and vertical cracks grew together and opened. At the same time, the vertical crack below the loading point grew into a flexural crack. After a significant increase in slip of the strands, the slabs collapsed.

The impact of the shear load on the fire behaviour is a paradox. On the one hand, the crack development and slip development is hardly affected by it. On the other hand, the shear load has a large influence on the time to failure. Apparently, the damage, i.e. cracking and slip, caused by the incompatible thermal expansion caused a large and rapid decrease of the load bearing capacity in the first 30 minutes. Hereafter the further decrease is small. A too high shear load leads to early failure whereas failure is postponed to 90 minutes and beyond when the shear load is sufficiently low.

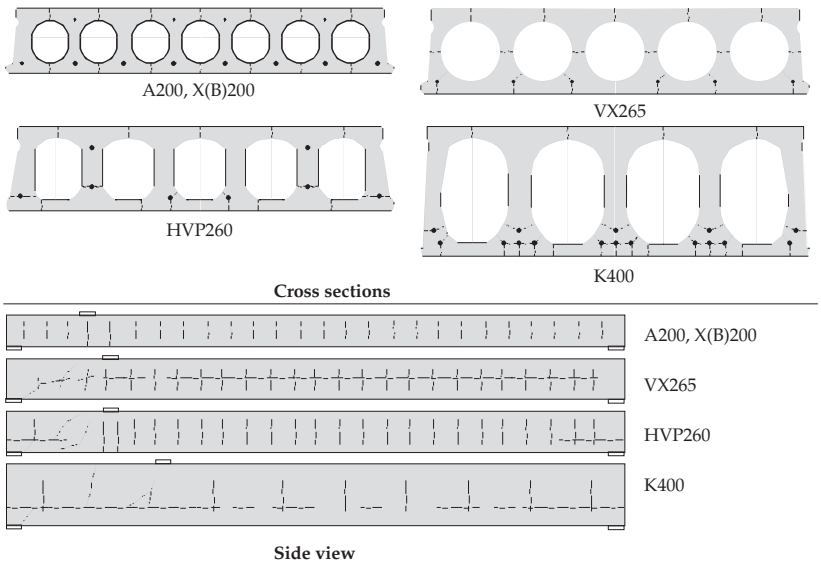

Figure 8. Sketch of the crack patterns for all slab geometries. The number in each type indication of the slabs indicates the depth of the slab

Restraining the thermal expansion in the spanning direction did not prevent the development of vertical cracks although the length of the cracks was shorter. The use of the reinforced end beam together with the reinforced core filling did not improve the fire performance. The results were very similar to the tests without this measure. This was attributed to the lack of bond between the core filling and the slabs that was observed after the test. Consequently, the tensile thermal stresses in the web could not spread out over the core filling. Although the lack of bond might be attributed to the preparation of the test-specimen only, it is uncertain to what extent the bond can be guaranteed in practical applications.

4 Numerical modelling

4.1 ***Formulation***

It was concluded from the test results that the splitting cracks, the vertical cracks and the slip development had to be included in the model for a realistic prediction of the actual behaviour. As splitting cracks result from circumferential tensile stresses around the strands in the cross section and vertical cracks result from tensile stresses in the spanning direction, a 3D model was required. However, in combination with the mesh refinement required to model the crack propagation near the crack tips, such a 3D model appeared to be beyond current computer capabilities. Therefore two separate plane stress models were developed in the FE package DIANA, one cross sectional model and a model of the entire slab including a bond-slip interface between the concrete and the strands, see Figure 9.

The cross sectional model was used for the determination of the temperature distribution during the fire assuming heating from the bottom side and taking into account radiative and convective heat transfer in the hollow cores. The conductivity and heat capacity of concrete and steel were obtained from the draft version of Eurocode 2 [9]as extensive research in the past showed that these values were satisfactory [5]. For the model of the entire slab, the temperatures were averaged over the width of the slab.

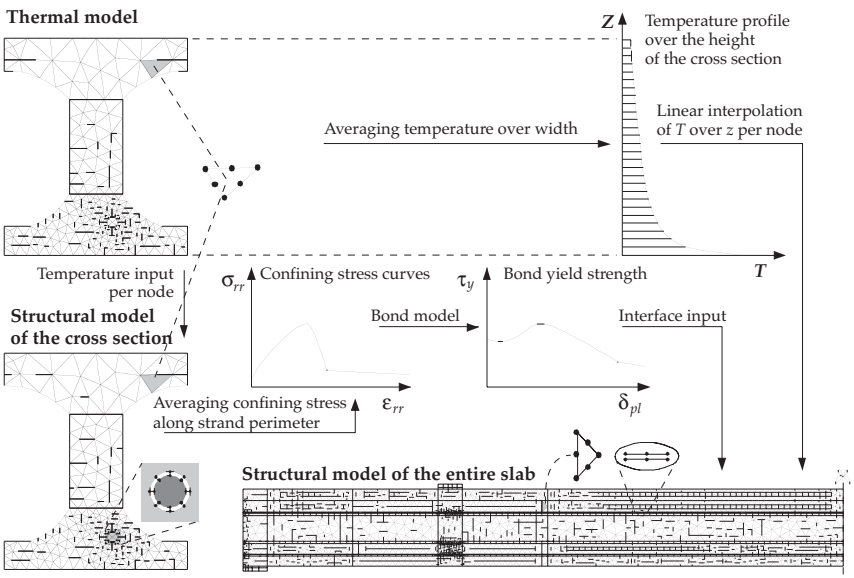

Figure 9. Overview of the modelling approach

Both structural models contained a new constitutive model for concrete, decomposing the strain increments into seven strain components, i.e. the thermal strain ε_T, shrinkage strain ε_s, elastic strain ε_{el}, plastic strain ε_{pl}, crack strain ε_{cr}, transient creep strain ε_{tr} and normal creep strain ε_{crp}:

$$\Delta\varepsilon = \Delta\varepsilon_T + \Delta\varepsilon_s + \Delta\varepsilon_{el} + \Delta\varepsilon_{pl} + \Delta\varepsilon_{cr} + \Delta\varepsilon_{tr} + \Delta\varepsilon_{crp} \qquad \text{eq. 2}$$

The thermal strain was taken from Eurocode 2 [16]. The shrinkage strain and normal creep strain were introduced to be able to predict the transfer of the prestress at the time of the release of the prestress in the production plant as well as possible. The formulations were approximated on the basis of the *fib* Bulletins [11]. The transient creep formulation was obtained from Anderberg and Thelandersson [2] which is standard available in the software used [7]. The elastic, plastic and crack strain were calculated using the Rankine – Drucker Prager yield model [7]. The softening branches in compression and tension were both based on fracture energy, allowing for localisation of deformations. The stress-strain relations in compression and tension depended on temperature and on the stress level during heating for compression. For the compression regime, these relations were based on an approximation of the results obtained from literature[18], [1], [17]. For the tensile regime they were based on the calibration tests described in § 4.2.

The model of the entire slab contained a newly developed constitutive model for the bond interface between the strands and the concrete embedment. It is an extension of the model for bond at room temperature developed by Den Uijl [19] with an elastic-plastic formulation and the effects of elevated temperature taken into account. The model decomposes the slip of the strand δ into an elastic part δ_{el} and a plastic part δ_{pl}, see Figure 10. The model assumes that the plastic part of the slip and a change in the steel strain ε_p of the strand lead to a fictitious radial expansion of the strand ε_{rr}. For various discrete time intervals (t_1, t_2,…) after casting of the slab, during curing and during fire exposure, the confining action of the concrete cover around the strand as a response to a fictitious radial expansion of the strand was calculated with the cross sectional model in terms of a confining stress σ_{rr}. The calculation included the effect of the non-linear temperature and thermal strain distribution and the development of splitting cracks. Through an adhesion-friction analogy, the bond yield strength tpl was related to the confining stress as calculated with the cross sectional model after averaging over the perimeter of the strand.

Due to the development of splitting cracks, the confining action depends on the history of radial expansion by releasing the prestress, loading and thermal effects. Cross sections near the end of the slab experience a completely different history than cross sections near mid span. This is because the release of the prestress only results in a slip and change of the steel strain

in cross sections near the end of the slab. To overcome this difference, each model of the entire slab was fed with confining stress curves that were calculated at 0, 5, 15, 30, 60 and 120 minutes of fire exposure for both a cross section without any initial radial expansion during the release of the prestress and for the cross section at the end of the slab with the maximum initial radial expansion during the release of the prestress. For cross sections with an intermediate initial radial expansion, the yield strength was obtained through linear interpolation.

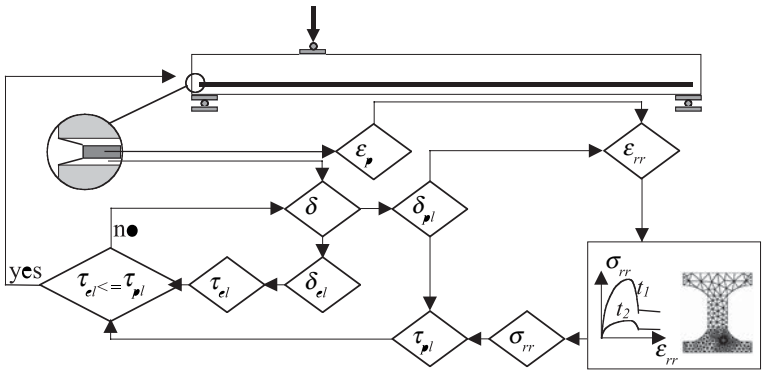

Figure 10. Overview of the constitutive bond model

4.2 ***Calibration***

The new constitutive models for concrete and the bond interface required calibration. For that purpose, a new test set up was developed, see Figure 11. The tensile strength and the fracture energy after cracking were determined for concrete at elevated temperatures of 20, 80, 150, 400 and 600 oC, using Brazilian splitting tests and pull-through tests respectively. The bond model parameters were determined with pull-out tests on strands embedded in small scale concrete cylinders at the same temperatures. In order to separate the contribution to the radial expansion of the strand by the slip and the change of the steel strain, pull-out tests were carried out with free and restrained passive end of the strand, see Figure 12. Each test was executed three times, resulting in a total of 60 tests.

First, the splitting force was measured in the Brazilian splitting tensile test. The tensile strength of concrete was deduced not only using a standard relation [13] between the splitting force and the tensile strength but also through inverse modelling using the FE model of the splitting test, in order to determine the effect of the non-linear stress-strain behaviour on the predicted splitting force. The non-linear stress-strain curve was obtained from Breunese [4].
Using again an inverse modelling technique, the fracture energy was calibrated at elevated temperatures. The confining stress as a function of the radial expansion was measured in the pull-through test. In this test, a conical bar is pulled through a slim concrete cylinder in which a conical central hole is cast. This results in a radial loading on the cylinder, leading to a curve

of the pulling force versus the displacement similar to the confining stress curve as indicated in Figure 9. The pulling force was related to the confining stress through a friction coefficient which was fixed by matching the peak values of the simulated confining stress curves to the peak value in the measured pulling force. With the confining stress curve and the tensile strength obtained in the splitting tests, the fracture energy of the concrete could be determined. Finally, the friction coefficient of the embedded strands was determined on the basis of the pull-out tests using both the obtained tensile strength and the fracture energy. The other bond parameters could also be calibrated using the pull-out tests, but with less accuracy.

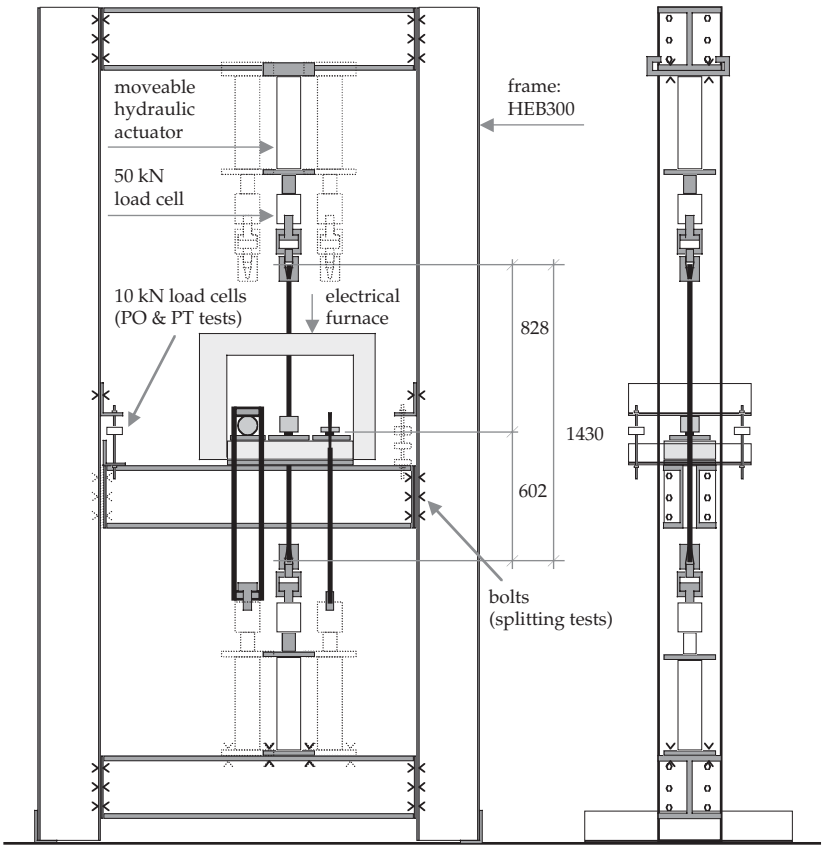

Figure 11. Newly developed test set up for the conduction of the calibration tests at elevated temperatures: splitting tensile tests (left specimen), pull-out (PO) tests (middle specimen) and pull-through (PT) tests (right specimen). In reality, opposite to what the figure suggests, only three identical specimen were installed in the furnace at the same time., since each type of test was carried out three times

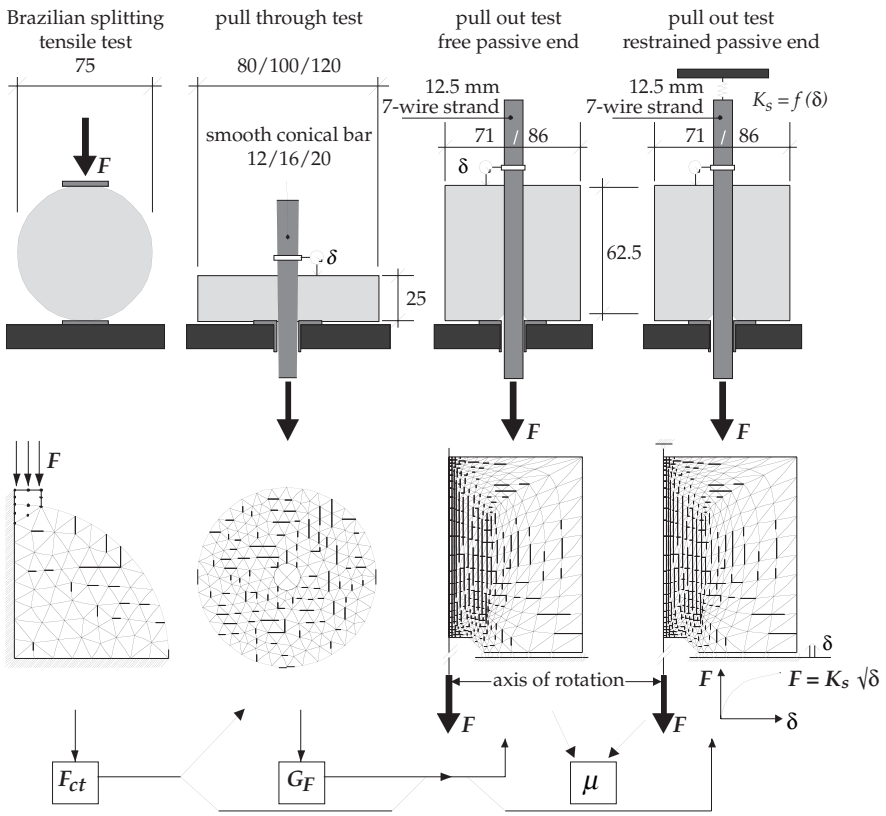

Figure 12. Overview of the types of specimen used in the calibration tests

4.3 ***Validation***

The FE models were validated against the fire tests described in § 3.3 using the calibrated material's properties. First, anchorage failure was simulated with the model of the entire slab for a 260 mm deep slab at room temperature, see Figure 13. A flexural crack is initiated at a loading of 109 kN at a distance of 690 mm from the slab end. Then, the load falls back and slip starts. At a load of 125 kN the maximum shear load is reached and the strand is pulled out. It is noted that the yield strength of the prestressing steel was assumed to be 2000 MPa, so no rupture of the strand occurred. Anchorage failure was properly calculated. In the tests, the slab failed at a load of 99 kN. The discrepancy between the measured and calculated shear load is attributed to the variations in the bond model parameters.

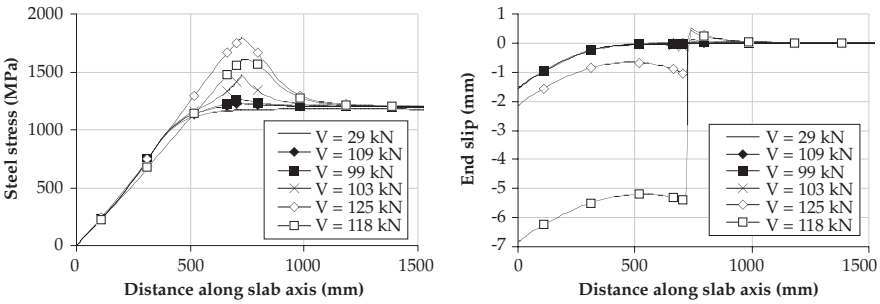

Figure 13. Development of steel stress (left) and slip (right) along the strand at various stages of shear loading

Both the splitting cracks and the vertical cracks could well be simulated by the model, see Figure 14. The horizontal cracks in the 265 mm deep slab at the smallest section of the web were properly simulated by the cross sectional model. The bottom flange tends to rotate due to the thermal gradient while the upper flange remains straight, resulting in a bending moment around the spanning direction, leading to tensile stresses in the web and finally cracking. If the upper flange would be thinner, the upper flange would crack rather than the web, see Figure 14.

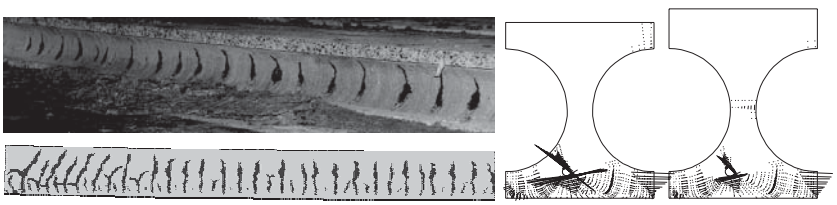

Figure 14. Comparison between experimental and simulated crack pattern in a 200 mm deep slab after 20 minutes (left) and horizontal cracking in the smallest section of the web of a 265 mm deep slab, depending on the thickness of the upper flange. Besides, large splitting cracks were calculated around the strand.

Also the simulated slip development of the strands is in acceptable agreement with the experimental results, see Figure 15. The figure shows that the slip development in the early stage of the fire is almost independent of the shear load, whereas the time to failure strongly depends on the shear load. The model follows the slip development rather well, although the time to failure is not calculated correctly. The difference in the time to failure is attributed to the sensitivity of the failure time to various influencing parameters, see next paragraph.

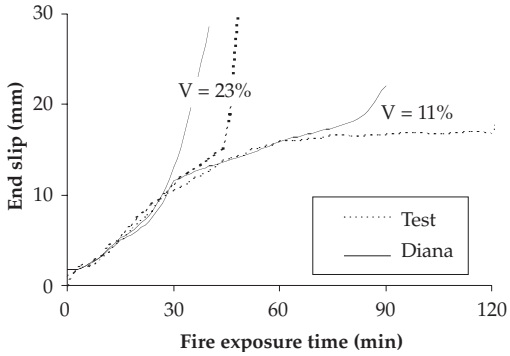

Figure 15. Comparison of the slip between the simulations with the FE model and two fire tests on double rib specimens of 260 mm depth, one test with 11 % and one test with 23 % shear load, relative to the actual capacity at room temperature

4.4 ***Evaluation***

With the validated models, a sensitivity study was carried out. The tensile strength, the fracture energy in tension and compression and the thermal expansion of the concrete were varied. It was demonstrated that the behaviour was almost identical for a mean tensile strength of 5 and 6 MPa. Also the fracture energy of the concrete in compression hardly affected the behaviour in terms of slip and crack development or time to failure.

However, the fracture energy of the concrete in tension and the thermal expansion have a strong influence on the fire behaviour, see fig. Figure 16. The type of aggregate determines largely the fracture energy [6] and the thermal expansion, as for instance is considered in the Eurocode [16]. If a less expanding aggregate is applied, like a calcareous concrete, the slip development and crack development lags behind concretes containing more expanding aggregates like siliceous aggregate or a mix of siliceous and calcareous aggregates which was used in Figure 16.

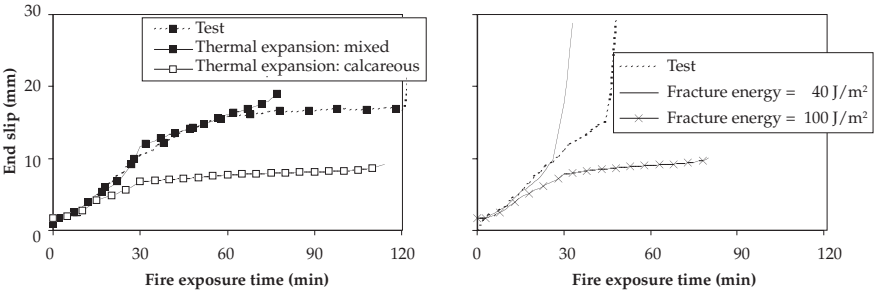

Figure 16. Effect on the slip development and the time to failure of the thermal expansion of concrete (left) and the fracture energy of concrete in tension (right) for a 260 mm deep double rib specimen

Finally, the effect of the loading history on the load bearing capacity will be discussed Calculations in which the load was kept constant until failure were compared with calculations in which no load was applied during heating and the load was increased up to failure at discrete time intervals, see Figure 17. It shows that the decrease of the load bearing capacity is very large in the early stage of the fire. But subsequently, the further decrease is small. It also shows that the decrease is almost irrespective to the applied load during fire.

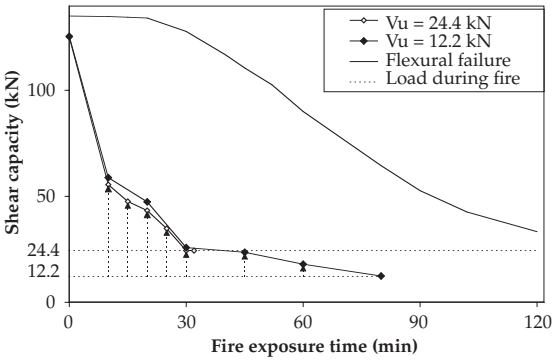

Figure 17. Decrease of the load bearing capacity during fire exposure as calculated with the FE models for two load levels during fire

With these calculations it was found that either the brittle or the ductile anchorage failure mode could govern the behaviour. At room temperature, the pull-out resistance of the strands was sufficient to take over the tensile stresses that are released at the initiation of a flexural crack., i.e. when the cracking moment resistance was reached. However, during the early stage of fire, the pull out resistance decreases more due to the splitting cracks than the cracking moment resistance due to the vertical cracks in the webs. As a result, the cracking moment resistance was limited by the anchorage capacity from 10 up to 30 to 60 minutes, leading to brittle failure. Hereafter the pull-out resistance is larger than the cracking moment resistance and anchorage failure is ductile again.

The difference in load bearing capacity after 30 minutes and 120 minutes is small when compared to the decrease of the flexural capacity., which is shown as well in figure 16. The decrease of the capacity to bear shear forces in the standard shear test limited by the flexural capacity is given. As a consequence, a HC slab designed for 120 minutes fire resistance has almost the same shear capacity as a HC slab designed for 60 minutes, whereas the flexural resistance will significantly differ. So, a fire resistance requirement of 120 minutes instead of 60 minutes hardly increases the safety level.

5 Conclusions and Recommendation

Current design codes like the new Eurocode 2 do not adequately take into account the shear and anchorage failure of fire exposed HC slabs. On the basis of 25 new fire tests and an in-depth investigation into existing fire test data on HC slabs, is was demonstrated that the shear and anchorage behaviour can lead to premature failure. Therefore, these failure modes should be considered in the fire design of HC slabs.

Incompatible thermal expansion leads to structural damage like cracking and slip of strands within 15 minutes of standard fire exposure. As a result, the shear and anchorage capacity strongly decrease in the early stage of fire, eventually leading to collapse, depending on the load level. As the decrease of the load bearing capacity is small after an early drop in the first 30 minutes of fire exposure, it is recommended to avoid shear and anchorage failure completely rather than to try to meet the required fire resistance time more precisely. In doing so, a desirable ductile failure will occur due to flexure. The shear and anchorage failure can be avoided by limiting the allowable shear load on the HC slab during fire. This maximum load can be determined for each HC slab on the market using the FE models presented in this paper.

The important influencing parameter is the type of aggregate. The type of aggregate determines the fracture energy of concrete and the thermal expansion of concrete. By monitoring and controlling these parameters in the design and production process, the allowable shear load can be maximised.

Furthermore, support conditions that restrain the thermal expansion overshadow other aspects. The amount of restraint that is needed to increase the allowable shear load to a desired level can also be determined with the FE models. However, the available restraint in a practical building is unknown and can yet not be guaranteed as it is very sensitive to the way the HC units are connected on site to the adjacent parts of the structure. Therefore it is recommended not to rely on such a beneficial effect while it can not be assured in the design.
If the effect of restraint is evaluated despite of the uncertainties involved in the practical applications, one should at least assume in testing and calculation that the fire is fully developed in the entire fire compartment. As the fire compartment comprises generally one entire storey in multi -storey buildings, the entire floor must be considered exposed to fire and consequently, restraint can only be generated through the rigidity of the vertical structure rather than by adjacent HC units. Fire tests that use restraint generated by adjacent floor slabs, are discouraged as those tests generally overestimate the restraint in real buildings and provide results at the unsafe side.

Finally, it is recommended to use the FE models to calculate for each type of HC slab on the market the maximum allowable shear load for which shear and anchorage failure is avoided. This results in a modification of the well known load-span interaction diagrams for these slabs. In doing so, no complex fire analyses need to be carried out in the design stage anymore, but a simple check of the load-span interaction diagram suffices to ensure an adequate safety level.

Acknowledgement

The authors wish to thank the Dutch technology foundation STW for it's financial support. Also the financial contributions by the concrete industry through the Union of Producers of Concrete Products in the Netherlands BFBN *(Bond van Fabrikanten van Betonproducten in Nederland)* and the steel industry through Building with Steel *(Bouwen met Staal)* is gratefully acknowledged. Finally, the authors wish to thank TNO Building and Construction Research for the facilitation of the research over the years by means of their experimental and computational infrastructure.

References

[1] Abrams, M.S. (1971), 'Compressive strength of concrete at temperatures to 1600 F' *in Temperature and Concrete*, ACI Special Publications SP25, Detroit, USA, pp 33-58

[2] Anderberg, Y, S. Thelandersson (1976), 'Stress and deformation characteristics of concrete at high temperatures, Part 2: Experimental investigation and material behaviour model', Lund: Lund University of Technology, Division of Structural Mechanics and Concrete Construction, Bull. 54

[3] Brekelmans, J.W.P.M., J.H.H. Fellinger, B.W.E.M. van Hove (1999), 'Aanbevelingen voor het ontwerp, de vervaardiging en toetsing van vloeren bestaande uit kanaalplaten met geïntegreerde stalen liggers', CUR-BmS rapport, Gouda, the Netherlands *(in Dutch)*

[4] Breunese, A.J. (2001) 'Tensile properties of concrete during fire', Rijswijk, TU Delft – TNO Centre for Fire Research report 2001-CVB-R04634

[5] Both, C. (1998), ''The fire resistance of composite steel concrete slabs', Dissertation TU Delft, Delft: Delft University Press

[6] Darwin, D., S. Barham, R. Kozul, S. Luan (2001), 'Fracture energy of high strength concrete', in *ACI Material's Journal*, Vol 98, Sep./Oct., pp 410-417

[7] DIANA (2003), 'DIANA Finite element analysis, user's manual, release 8.1', Delft: TNO

[8] ECCS Publication 103 (1998), 'Guidelines for the application of prestressed hollow core slabs supported on built-in beams', Brussels: ECCS

[9] ENV1992-1-2 (1995), 'Eurocode 2: Design of concrete structures, Part 1.2: General rules, structural fire design', Brussels: CEN

[10] Fellinger, J.H.H. (2004), 'Shear and anchorage behaviour of fire exposed hollow core slabs', Dissertation TU Delft, Delft: Delft University Press

[11] FIB (1999), 'Structural concrete, textbook on behaviour, design and performance', *fib* manual bulletin 1, Lausanne: FIB.

[12] Model Code 1990 (1991), 'Design code for concrete structures', Trowbridge: Thomas Telford

[13] NEN 5959 (1997), 'Beton en mortel – Bepaling van de splijttreksterkte van proefstukken', Delft: NEN *(in Dutch)*

[14] ISO 834-1 (1999), 'Fire resistance tests, elements for building construction – Part 1: General requirements', Geneva: ISO

[15] prEN1168-1 (1997), 'Pre-cast concrete products - Hollow core slabs for floors – Part 1, Pre-stressed slabs', Brussels: CEN

[16] prEN1992-1-2 (2002), 'Eurocode 2: Design of concrete structures, Part 1.2 General rules, Structural fire design', Brussels: CEN

[17] Purkiss, J.A., A. Bali (1988), 'The transient behaviour of concrete at temperatures up to 800 ºC', in *Proceedings of the 10th Ibausil Weimar 1988, Hochschule für Architectur und Bauwesen*, Weimar, pp. 234-239

[18] Schneider, U. (1988), 'Concrete at high temperature – A general review', in *Fire Safety Journal*, Vol. 13, pp 55-68

[19] den Uijl, J.A. (1998), 'Bond modelling of prestressing strand', in *ACI Special Publication 180*, Michigan USA, pp 145-169

[20] Walraven, J.C., P. Mercx (1983), 'The bearing capacity of prestressed hollow core slabs', in *Heron* Vol. 28 – No. 3